J. Fluid Mech. (1976), *vol.* 77, *part* 1, *pp.* 45–62
Printed in Great Britain

Bispectral measurements in turbulence

By K. S. LII, M. ROSENBLATT AND C. VAN ATTA
University of California, La Jolla

(Received 13 August 1975 and in revised form 26 April 1976)

A bispectral analysis of high Reynolds number turbulent velocity-derivative data is carried out. The computations suggest that contributions of wavenumber triplets to the rate of vorticity production and spectral transfer are non-local in wavenumber space and comparable over the whole range of wavenumbers studied. Statistical resolvability of the bispectral estimates is obtained. An appendix on the asymptotic behaviour of bispectral estimates is given.

1. Introduction

The bispectrum has been used in a number of investigations as a tool. We mention in particular the work of Hasselman, Munk & MacDonald (1963) on ocean waves, the paper of Brillinger & Rosenblatt (1967) on sunspots, that of Cartwright (1968) on tides, an application of Huber *et al.* (1971) analysing EEG readings and the study of Roden & Bendiner (1973) on profiles of oceanographic variables. The analysis of data in these papers was helpful but did not lead to strong new insight. There have also been large sample theoretical investigations of bispectral estimates, which are described, for example, in Brillinger & Rosenblatt (1967) and Rosenblatt (1971). In this paper, the insight that accurate bispectral estimates in turbulence could provide in the analysis of energy transfer and dissipation is considered at some length. Hot-wire data obtained from an experiment carried out during an atmospheric measurement programme described by Haugen, Kaimal & Bradley (1971) is used to obtain a bispectral estimate with effective statistical resolution. The results are promising in that they give some more effective insight here than in the earlier attempts in other areas described above. There are also further experimental measurement programmes that are naturally suggested which would provide data for further supplementary attempts at bispectral estimation that would give a more complete picture. An appendix on higher-order spectra relating to their estimation is included.

2. Energy dissipation and energy transfer

As pointed out by Taylor (1938), the physical mechanism of dissipation of turbulent kinetic energy is associated with the stretching of vortex lines. Thus, in homogeneous turbulence

$$\epsilon = \nu E\{\boldsymbol{\omega}^2\}\dagger \tag{1}$$

† The operator E denotes 'the mean of'.

and the decay of kinetic energy corresponds to the production of fluctuating vorticity $\boldsymbol{\omega}$.

The equation for the rate of increase of $E\{\boldsymbol{\omega}^2\}$, first given by von Kármán (1937), is

$$\frac{\partial}{\partial t} E\{\boldsymbol{\omega}^2\} = E\left\{\omega_i \omega_j \frac{\partial u_i}{\partial x_j}\right\} - \nu E\left(\frac{\partial \omega_i}{\partial x_j}\right)^2, \tag{2}$$

where u is the velocity. The standard summation convention is used, i.e. summation over all values of an index if it appears twice. The first term on the right-hand side of (2) describes the rate of amplification of vorticity by stretching of vortex lines, while the second describes the rate of viscous decay of the fluctuating vorticity. For homogeneous turbulence, the stretching term is related to the mean value of the principal rates of strain in the fluid (Batchelor & Townsend 1956; Betchov 1956) by the relation

$$E\{\omega_i \omega_j \partial u_i/\partial x_j\} = -4E\{abc\}, \tag{3}$$

where a, b and c are the eigenvalues of the symmetric rate-of-strain tensor $\{\partial u_i/\partial x_j + \partial u_j/\partial x_i\}$.

If the turbulence is also isotropic, then

$$E\{abc\} = \frac{35}{8} E\left(\frac{\partial u}{\partial x}\right)^3 = \frac{35}{8} S \frac{\{Eu^2\}^{\frac{3}{2}}}{\lambda^3}, \tag{4}$$

where

$$S = E\left(\frac{\partial u}{\partial x}\right)^3 \Big/ \left\{E\left(\frac{\partial u}{\partial x}\right)^2\right\}^{\frac{3}{2}}$$

is the skewness factor of $\partial u/\partial x$ and

$$\lambda = \left\{Eu^2/E\left(\frac{\partial u}{\partial x}\right)^2\right\}^{\frac{1}{2}}$$

is the Taylor microscale. From (2) a necessary requirement for a balance of vorticity production and destruction is that $S < 0$.

For isotropic turbulence the spectral density of $E\{\boldsymbol{\omega}^2\}$ is $2k^2 f(k)$, where $f(k)$ is the three-dimensional energy spectrum, so that the principal contribution to $E\{\boldsymbol{\omega}^2\}$ comes from larger wavenumbers. The production of vorticity is associated with a transfer of spectral energy from small wavenumbers to large wavenumbers produced by the mechanism of vortex stretching. In wavenumber space, the transfer is described in terms of interactions between triplets of wavenumbers whose wave vectors sum to zero. The question naturally arises as to what wavenumber triplets are interacting most strongly to produce the dominant contributions to the spectral transfer and production of vorticity. For the present situation, the natural tool for investigating this question is the bispectrum of $\partial u/\partial x$, i.e. $B'(k_1, k_2)$. Since we shall be dealing only with the usual one-dimensional experimental sampling of the turbulent field, in the following our wavenumber k will be understood to refer only to the longitudinal wavenumber associated with the direction of the mean velocity. Then

$$B'(k_1, k_2) = \frac{1}{(2\pi)^2} \int\int_{-\infty}^{\infty} E\left\{\frac{\partial u}{\partial x}(x) \frac{\partial u}{\partial x}(x+r_1) \frac{\partial u}{\partial x}(x+r_2)\right\} \exp\{-ik_1 r_1 - ik_2 r_2\} dr_1 dr_2 \tag{5}$$

and

$$E\left\{\frac{\partial u}{\partial x}(x)\frac{\partial u}{\partial x}(x+r_1)\frac{\partial u}{\partial x}(x+r_2)\right\} = \iint_{-\infty}^{\infty} B'(k_1, k_2)\exp\{ik_1 r_1 + ik_2 r_2\}\,dk_1\,dk_2. \quad (6)$$

The bispectrum $B'(k_1, k_2)$ gives the contribution to the mean cube of $\partial u/\partial x$ from wavenumber triplets k_1, k_2, k_3 for which $k_1+k_2+k_3 = 0$. Setting r_1 and r_2 equal to zero in (6) and noting that $E(\partial u/\partial x)^3$ is real suggests that $B'(k_1, k_2)$, the bispectrum of $\partial u/\partial x$, might be real. $B'(k_1, k_2)$ is related to the bispectrum $B(k_1, k_2)$ of $u(x)$ by

$$B'(k_1, k_2) = -ik_1 k_2(k_1+k_2)\,B(k_1,\ k_2). \quad (7)$$

Let us assume that we have a velocity field $\mathbf{u}(\mathbf{x}, t)$ of homogeneous turbulence as in Batchelor (1953). If the Navier–Stokes equation is satisfied

$$\partial\mathbf{u}/\partial t + \mathbf{u}.\nabla\mathbf{u} = -\rho^{-1}\nabla p + \nu\nabla^2\mathbf{u}, \quad (8)$$

where p is the pressure, ρ the density and ν the kinematic viscosity. Given incompressibility, the continuity equation becomes

$$\nabla.\mathbf{u} = 0. \quad (9)$$

Throughout the paper, appropriate moments are assumed to exist. The homogeneity of the field implies that one can carry out a spatial harmonic analysis

$$\mathbf{u}(\mathbf{x}, t) = \int e^{i\mathbf{k}.\mathbf{x}} d\mathbf{z}(\mathbf{k}, t), \quad (10)$$

where $\mathbf{z}(\mathbf{k}) = \mathbf{z}(\mathbf{k}, t)$ is a process of orthogonal increments in $\mathbf{k}$.

The dynamical equation for $f_{ii}(\mathbf{k})$, the spectral energy density associated with a wave vector $\mathbf{k}$, is (Batchelor 1953, p. 85)

$$\frac{\partial}{\partial t}[\tfrac{1}{2}f_{ii}(\mathbf{k})] = \int Q(\mathbf{k}, \mathbf{k}')\,d\mathbf{k}' - \nu\mathbf{k}^2 f_{ii}(\mathbf{k}), \quad (11)$$

where $$Q_{\alpha,\beta}(\mathbf{k}, \mathbf{k}')\,dk\,dk' = \operatorname{Im} E\{k_\alpha\,dz_\alpha(\mathbf{k}-\mathbf{k}')\,dz_\beta(-\mathbf{k})\,dz_\beta(\mathbf{k}')\} \quad (12)$$

($d\mathbf{z}^*(\mathbf{k}) = d\mathbf{z}(-\mathbf{k})$ since the velocity field has real components) and

$$Q(\mathbf{k}, \mathbf{k}') = \sum_{\alpha,\beta} Q_{\alpha,\beta}(\mathbf{k}, \mathbf{k}').$$

$Q(\mathbf{k}, \mathbf{k}')$ can be interpreted as the mean rate of transfer of energy from $d\mathbf{k}'$ to $d\mathbf{k}$. The continuity equation implies that

$$Q(\mathbf{k}, \mathbf{k}') + Q(\mathbf{k}', \mathbf{k}) = 0.$$

As shown by Yeh & Van Atta (1973, equation 12),

$$Q(\mathbf{k}, \mathbf{k}') = -k_l \operatorname{Im}[B_{l,n,n}(\mathbf{k}, -\mathbf{k}')], \quad (13)$$

where $B_{l,n,n}(\mathbf{k}, \mathbf{k}')$ is the three-dimensional bispectrum of the velocity field and l and n denote the direction of the velocity component chosen at each of the three points (see Yeh & Van Atta 1973, equation 8). Our one-dimensional bispectrum for the u component, $B(k_1, k_1')$, is given in terms of one component of $B_{l,n,n}(\mathbf{k}, \mathbf{k}')$ by the relation

$$B(k_1, k_1') = \iint B_{1,1,1}(\mathbf{k}, \mathbf{k}')\,dk_\alpha\,dk_\beta\,dk_\alpha'\,dk_\beta'.$$

Here k_α and k_β refer to the k_2 and k_3 axes in $\mathbf{k}$ space, while, following the convention adopted here, k_1 and k_1' are two wavenumbers associated with the k_1 axis in $\mathbf{k}$ space. The measured bispectrum of u or $\partial u/\partial k$ gives information about only one of the nine bispectral terms in $Q(\mathbf{k}, \mathbf{k}')$.

An equation similar to (12) with one-dimensional wavenumbers instead of wave vectors as variables can also be derived. Let

$$g_{ii}(k_1) = \iint f_{ii}(k_1, k_2, k_3)\, dk_2\, dk_3, \tag{14a}$$

$$h_2(k_1) = \iint k_2^2 f_{ii}(k_1, k_2, k_3)\, dk_2\, dk_3, \tag{14b}$$

$$h_3(k_1) = \iint k_3^2 f_{ii}(k_1, k_2, k_3)\, dk_2\, dk_3 \tag{14c}$$

and
$$q_{\alpha,\beta}(k_1, k_1') = \iint Q_{\alpha,\beta}(k_1, k_2, k_3, k_1', k_2', k_3')\, dk_2\, dk_3\, dk_2'\, dk_3', \tag{15}$$

with
$$q(k_1, k_1') = \sum_{\alpha,\beta} q_{\alpha,\beta}(k_1, k_1').$$

One can show that

$$\operatorname{Re} B'(k_1, k_1') = k_1'(k_1 + k_1')\, q_{1,1}(k_1, k_1'),$$

where $\mathbf{k} = (k_1, k_2, k_3)$ and $\mathbf{k}' = (k_1', k_2', k_3')$. Then

$$\frac{\partial}{\partial t}[\tfrac{1}{2} g_{ii}(k_1)] = \int q(k_1, k_1')\, dk_1' - \nu k_1^2 g_{ii}(k_1) - \nu h_2(k_1) - \nu h_3(k_1). \tag{16}$$

In (12) one of the terms is

$$\operatorname{Im}\{k_1 E\{dz_1(\mathbf{k}-\mathbf{k}')\, dz_1(-\mathbf{k})\, dz_1(\mathbf{k}')\}\}.$$

Let us integrate this over k_2, k_3, k_2' and k_3'. The resulting expression except for the factor k_1 is proportional to the imaginary part of the one-dimensional velocity bispectrum. We have estimated the velocity-derivative bispectrum, which is related to the velocity bispectrum by (7). Looking at the velocity derivative acts as a sort of prewhitening, damps out the very low frequency bispectral mass and prevents it from leaking and masking the bispectral mass away from zero. This one-dimensional velocity bispectrum is one of the various terms appearing in $q(k_1, k_1')$. It would be of considerable interest to estimate some of the other terms and see whether they agree with the symmetries one would anticipate in the case of isotropy.

The assumption underlying the Kolmogorov wavenumber-cascade idea of spectral energy transfer is that most of the important interactions are local in wavenumber space. In his (1959) paper, Kraichnan considers a model in which spectral energy transport throughout the inertial and dissipation ranges is found to proceed by a cascade process essentially local in wavenumber space. In a later paper (1971) Kraichnan comments that in three dimensions the transfer is already not very local, and this is strongly suggested by the analysis of experimental data we have carried out. If the dominant interactions were very localized one would expect to find a rather peaked bispectrum along a diagonal and we find (see § 5 and tables 1, 3 and 5) that this is not the case. Notice that symmetries imply that $B(k_1, k_1') = B(k_1', k_1) = B(k_1, -k_1 - k_1')$.

3. Data acquisition and processing

The data were obtained from a modest hot-wire experiment carried out during the atmospheric-surface-layer measurement programme described by Haugen *et al.* (1971). The basic data for the streamwise velocity derivative used in the present measurements were part of the data used in previous studies by Van Atta & Yeh (1973, 1975) and by Wyngaard & Pao (1972). A single vertically oriented hot wire 5 μm in diameter and 1·2 mm long was operated in the linearized constant-temperature mode (DISA 55D05-15 unit) at a height of $z = 5{\cdot}66$ m. The mean velocity U was 3·78 m/s and the Komogorov microscale η was 0·08 cm. The streamwise velocity derivative $\partial u/\partial t$ was obtained from a four-pole Butterworth filter (Wyngaard & Lumley 1967), which differentiated and low-pass filtered (24 dB per octave) the u signal from the anemometer to eliminate high frequency noise. This signal was then recorded on analog magnetic tape. The previous studies which used the same basic data provide further details of the data acquisition and estimates of the accuracy of the data. The analog data were played back in the laboratory of the Department of Applied Mechanics and Engineering Sciences, UCSD, sampled with a 12-bit analog-to-digital converter at a sample rate of 4172 samples per second, and written on digital magnetic tape. The skewness factor S of the derivative $\partial u/\partial t$ is $-0{\cdot}85438$.

4. Computation

The computation was done by using a CDC 7600 digital computer in Lawrence Berkeley Laboratory at Berkeley through a terminal in the Institute of Geophysics and Planetary Physics at La Jolla. The digital tape consisted of 700 records, each record containing 8192 values of $\partial u/\partial t$ in approximately 2 s of real time. There is a small gap between each record. The procedures used to compute the bispectrum were as follows.

(1) To reduce the effect of aliasing, the data were pre-filtered by averaging every eight readings. The resulting 1024 readings in each record are denoted by $x_1, x_2, \ldots, x_{1024}$.

(2) Each record was fast Fourier transformed and the mean of each record was removed, i.e. we computed

$$F(\lambda) = \sum_{j=1}^{n} \exp(ij\lambda 2\pi/n)\, x_j, \quad \lambda = 0, 1, \ldots, n-1, \quad n = 1024,$$

and set $F(0) = 0$. Note that by symmetry we only need to compute $F(\lambda)$ for $\lambda = 0, 1, 2, \ldots, 512$.

(3) The bispectrum estimate

$$b(\lambda_1, \lambda_2) = (2\pi)^{-2} n^{-1} F(\lambda_1)\, F(\lambda_2)\, F(-\lambda_1 - \lambda_2), \quad \lambda_1, \lambda_2 = 0, 1, \ldots, 330,$$

was computed for each record. Note that we did not compute this for the full range of (λ_1, λ_2) owing to the limitation of the memory of the CDC 7600, the primary interest in the inertial range and the cost of computation. The largest array we could use had 131071 words.

Frequency	0	1	2	3	4	5	6	7	8	9
0	$-2{\cdot}58\times10^{3}$	$-4{\cdot}84\times10^{3}$	$-5{\cdot}25\times10^{3}$	$-3{\cdot}45\times10^{3}$	$-2{\cdot}06\times10^{3}$	$-2{\cdot}36\times10^{3}$	$-3{\cdot}45\times10^{3}$	$-2{\cdot}11\times10^{3}$	$-3{\cdot}15\times10^{3}$	$-3{\cdot}10\times10^{3}$
	$(6{\cdot}34\times10^{2})$	$(1{\cdot}06\times10^{3})$	$(9{\cdot}69\times10^{2})$	$(7{\cdot}27\times10^{2})$	$(1{\cdot}10\times10^{3})$	$(1{\cdot}02\times10^{3})$	$(1{\cdot}19\times10^{3})$	$(1{\cdot}19\times10^{3})$	$(9{\cdot}15\times10^{2})$	$(1{\cdot}04\times10^{3})$
1	$-4{\cdot}84\times10^{3}$	$-3{\cdot}83\times10^{3}$	$-6{\cdot}74\times10^{3}$	$-4{\cdot}51\times10^{3}$	$-6{\cdot}06\times10^{3}$	$-4{\cdot}78\times10^{3}$	$-5{\cdot}24\times10^{3}$	$-4{\cdot}84\times10^{3}$	$-2{\cdot}55\times10^{3}$	$-4{\cdot}92\times10^{3}$
	$(1{\cdot}06\times10^{2})$	$(1{\cdot}18\times10^{3})$	$(1{\cdot}01\times10^{3})$	$(1{\cdot}01\times10^{3})$	$(1{\cdot}28\times10^{3})$	$(8{\cdot}98\times10^{2})$	$(9{\cdot}99\times10^{2})$	$(1{\cdot}02\times10^{2})$	$(8{\cdot}66\times10^{2})$	$(1{\cdot}05\times10^{3})$
2	$-5{\cdot}25\times10^{3}$	$-6{\cdot}74\times10^{3}$	$-4{\cdot}48\times10^{3}$	$-5{\cdot}22\times10^{3}$	$-2{\cdot}11\times10^{3}$	$-5{\cdot}68\times10^{3}$	$-3{\cdot}79\times10^{3}$	$-3{\cdot}64\times10^{3}$	$-5{\cdot}55\times10^{3}$	$-4{\cdot}22\times10^{3}$
	$(9{\cdot}69\times10^{2})$	$(1{\cdot}01\times10^{3})$	$(1{\cdot}50\times10^{3})$	$(1{\cdot}16\times10^{3})$	$(1{\cdot}20\times10^{3})$	$(1{\cdot}43\times10^{3})$	$(1{\cdot}09\times10^{3})$	$(8{\cdot}77\times10^{2})$	$(1{\cdot}27\times10^{3})$	$(7{\cdot}61\times10^{2})$
3	$-3{\cdot}45\times10^{3}$	$-4{\cdot}51\times10^{3}$	$-5{\cdot}22\times10^{3}$	$-7{\cdot}29\times10^{3}$	$-4{\cdot}29\times10^{3}$	$-4{\cdot}06\times10^{3}$	$-3{\cdot}52\times10^{3}$	$-3{\cdot}04\times10^{3}$	$-2{\cdot}32\times10^{3}$	$-2{\cdot}82\times10^{3}$
	$(7{\cdot}27\times10^{2})$	$(1{\cdot}01\times10^{3})$	$(1{\cdot}16\times10^{3})$	$(1{\cdot}62\times10^{3})$	$(1{\cdot}01\times10^{3})$	$(1{\cdot}30\times10^{3})$	$(9{\cdot}72\times10^{2})$	$(1{\cdot}54\times10^{3})$	$(1{\cdot}02\times10^{3})$	$(1{\cdot}17\times10^{3})$
4	$-2{\cdot}06\times10^{3}$	$-6{\cdot}06\times10^{3}$	$-2{\cdot}11\times10^{3}$	$-4{\cdot}29\times10^{3}$	$-6{\cdot}43\times10^{3}$	$-3{\cdot}43\times10^{3}$	$-3{\cdot}03\times10^{3}$	$-2{\cdot}02\times10^{3}$	$-2{\cdot}91\times10^{3}$	$-2{\cdot}53\times10^{3}$
	$(1{\cdot}10\times10^{3})$	$(1{\cdot}28\times10^{3})$	$(1{\cdot}20\times10^{3})$	$(1{\cdot}01\times10^{3})$	$(2{\cdot}17\times10^{3})$	$(1{\cdot}28\times10^{3})$	$(9{\cdot}60\times10^{2})$	$(1{\cdot}33\times10^{3})$	$(1{\cdot}07\times10^{3})$	$(1{\cdot}20\times10^{3})$
5	$-2{\cdot}36\times10^{3}$	$-4{\cdot}78\times10^{3}$	$5{\cdot}68\times10^{3}$	$-4{\cdot}06\times10^{3}$	$-3{\cdot}43\times10^{3}$	$-2{\cdot}62\times10^{3}$	$-5{\cdot}23\times10^{3}$	$-4{\cdot}33\times10^{3}$	$-3{\cdot}30\times10^{3}$	$2{\cdot}13\times10^{3}$
	$(1{\cdot}02\times10^{3})$	$(8{\cdot}98\times10^{2})$	$(1{\cdot}43\times10^{3})$	$(1{\cdot}30\times10^{3})$	$(1{\cdot}28\times10^{3})$	$(1{\cdot}81\times10^{3})$	$(1{\cdot}19\times10^{3})$	$(1{\cdot}35\times10^{3})$	$(1{\cdot}20\times10^{3})$	$(1{\cdot}30\times10^{3})$
6	$-3{\cdot}45\times10^{3}$	$-5{\cdot}24\times10^{3}$	$-3{\cdot}79\times10^{3}$	$-3{\cdot}52\times10^{3}$	$-3{\cdot}03\times10^{3}$	$-5{\cdot}23\times10^{3}$	$-4{\cdot}76\times10^{3}$	$-4{\cdot}73\times10^{3}$	$-1{\cdot}70\times10^{3}$	$-2{\cdot}49\times10^{3}$
	$(1{\cdot}19\times10^{3})$	$(9{\cdot}99\times10^{2})$	$(1{\cdot}09\times10^{3})$	$(9{\cdot}72\times10^{2})$	$(9{\cdot}60\times10^{2})$	$(1{\cdot}19\times10^{3})$	$(1{\cdot}44\times10^{3})$	$(1{\cdot}31\times10^{3})$	$(1{\cdot}54\times10^{3})$	$(1{\cdot}11\times10^{3})$
7	$-2{\cdot}11\times10^{3}$	$-4{\cdot}84\times10^{3}$	$-3{\cdot}64\times10^{3}$	$-3{\cdot}04\times10^{3}$	$-2{\cdot}02\times10^{3}$	$-4{\cdot}33\times10^{3}$	$-4{\cdot}73\times10^{3}$	$-3{\cdot}17\times10^{3}$	$-3{\cdot}31\times10^{3}$	$-2{\cdot}48\times10^{3}$
	$(1{\cdot}19\times10^{3})$	$(1{\cdot}02\times10^{3})$	$(8{\cdot}77\times10^{2})$	$(1{\cdot}54\times10^{3})$	$(1{\cdot}33\times10^{3})$	$(1{\cdot}35\times10^{3})$	$(1{\cdot}31\times10^{3})$	$(1{\cdot}66\times10^{3})$	$(1{\cdot}23\times10^{3})$	$(9{\cdot}63\times10^{2})$
8	$-3{\cdot}15\times10^{3}$	$-2{\cdot}55\times10^{3}$	$-5{\cdot}55\times10^{3}$	$-2{\cdot}32\times10^{3}$	$-2{\cdot}91\times10^{3}$	$-3{\cdot}30\times10^{3}$	$-1{\cdot}70\times10^{3}$	$-3{\cdot}31\times10^{3}$	$-3{\cdot}92\times10^{3}$	$-2{\cdot}27\times10^{3}$
	$(9{\cdot}15\times10^{2})$	$(8{\cdot}66\times10^{2})$	$(1{\cdot}27\times10^{3})$	$(1{\cdot}02\times10^{3})$	$(1{\cdot}07\times10^{3})$	$(1{\cdot}20\times10^{3})$	$(1{\cdot}54\times10^{3})$	$(1{\cdot}22\times10^{3})$	$(1{\cdot}77\times10^{3})$	$(1{\cdot}45\times10^{3})$
9	$-3{\cdot}10\times10^{3}$	$-4{\cdot}92\times10^{3}$	$-4{\cdot}22\times10^{3}$	$-2{\cdot}82\times10^{3}$	$-2{\cdot}53\times10^{3}$	$-2{\cdot}13\times10^{3}$	$-2{\cdot}49\times10^{3}$	$-2{\cdot}48\times10^{3}$	$-2{\cdot}27\times10^{3}$	$-1{\cdot}23\times10^{3}$
	$(1{\cdot}04\times10^{3})$	$(1{\cdot}05\times10^{3})$	$(7{\cdot}61\times10^{2})$	$(1{\cdot}17\times10^{3})$	$(1{\cdot}20\times10^{3})$	$(1{\cdot}30\times10^{3})$	$(1{\cdot}11\times10^{3})$	$(9{\cdot}63\times10^{2})$	$(1{\cdot}45\times10^{3})$	$(1{\cdot}29\times10^{3})$

TABLE 1. Estimated real part of bispectrum of velocity derivative (record 301–400). Estimated standard deviation in parentheses. One unit in frequency is 15·276 Hz.

Frequency	0	1	2	3	4	5	6	7	8	9
0	$1{\cdot}56\times10^{2}$ $(4{\cdot}93\times10^{2})$	$4{\cdot}45\times10^{1}$ $(2{\cdot}38\times10^{2})$	$8{\cdot}88\times10^{1}$ $(3{\cdot}36\times10^{2})$	$3{\cdot}01\times10^{2}$ $(3{\cdot}00\times10^{2})$	$-6{\cdot}56\times10^{2}$ $(3{\cdot}34\times10^{2})$	$6{\cdot}01\times10^{2}$ $(3{\cdot}38\times10^{2})$	$-4{\cdot}63\times10^{2}$ $(2{\cdot}72\times10^{2})$	$5{\cdot}37\times10^{2}$ $(3{\cdot}08\times10^{2})$	$-4{\cdot}56\times10^{2}$ $(2{\cdot}88\times10^{2})$	$-5{\cdot}95\times10^{1}$ $(2{\cdot}92\times10^{2})$
1	$4{\cdot}45\times10^{1}$ $(2{\cdot}38\times10^{2})$	$-2{\cdot}71\times10^{3}$ $(9{\cdot}84\times10^{2})$	$-2{\cdot}20\times10^{3}$ $(1{\cdot}02\times10^{3})$	$3{\cdot}99\times10^{2}$ $(9{\cdot}52\times10^{2})$	$-1{\cdot}09\times10^{3}$ $(1{\cdot}03\times10^{3})$	$1{\cdot}14\times10^{3}$ $(1{\cdot}08\times10^{3})$	$-2{\cdot}87\times10^{-1}$ $(1{\cdot}00\times10^{3})$	$2{\cdot}29\times10^{3}$ $(1{\cdot}14\times10^{3})$	$6{\cdot}80\times10^{2}$ $(1{\cdot}14\times10^{3})$	$9{\cdot}86\times10^{2}$ $(7{\cdot}84\times10^{2})$
2	$8{\cdot}88\times10^{1}$ $(3{\cdot}36\times10^{2})$	$-2{\cdot}20\times10^{3}$ $(1{\cdot}02\times10^{3})$	$7{\cdot}32\times10^{2}$ $(1{\cdot}79\times10^{3})$	$2{\cdot}26\times10^{3}$ $(1{\cdot}55\times10^{3})$	$3{\cdot}20\times10^{3}$ $(1{\cdot}20\times10^{3})$	$-9{\cdot}99\times10^{2}$ $(1{\cdot}26\times10^{3})$	$-9{\cdot}07\times10^{2}$ $(1{\cdot}26\times10^{3})$	$1{\cdot}18\times10^{3}$ $(1{\cdot}16\times10^{3})$	$1{\cdot}00\times10^{3}$ $(9{\cdot}82\times10^{2})$	$1{\cdot}67\times10^{2}$ $(1{\cdot}04\times10^{3})$
3	$3{\cdot}01\times10^{2}$ $(3{\cdot}00\times10^{2})$	$3{\cdot}99\times10^{2}$ $(9{\cdot}52\times10^{2})$	$2{\cdot}26\times10^{3}$ $(1{\cdot}55\times10^{3})$	$1{\cdot}21\times10^{3}$ $(1{\cdot}90\times10^{3})$	$5{\cdot}77\times10^{2}$ $(1{\cdot}32\times10^{3})$	$2{\cdot}21\times10^{3}$ $(1{\cdot}57\times10^{3})$	$3{\cdot}23\times10^{3}$ $(1{\cdot}66\times10^{3})$	$2{\cdot}53\times10^{3}$ $(1{\cdot}29\times10^{3})$	$2{\cdot}02\times10^{3}$ $(9{\cdot}67\times10^{2})$	$7{\cdot}58\times10^{2}$ $(9{\cdot}78\times10^{2})$
4	$-6{\cdot}56\times10^{2}$ $(3{\cdot}34\times10^{2})$	$-1{\cdot}09\times10^{3}$ $(1{\cdot}03\times10^{3})$	$3{\cdot}20\times10^{3}$ $(1{\cdot}20\times10^{3})$	$5{\cdot}77\times10^{2}$ $(1{\cdot}32\times10^{3})$	$2{\cdot}42\times10^{3}$ $(1{\cdot}94\times10^{3})$	$1{\cdot}27\times10^{3}$ $(1{\cdot}39\times10^{3})$	$8{\cdot}39\times10^{2}$ $(1{\cdot}30\times10^{3})$	$-1{\cdot}83\times10^{3}$ $(1{\cdot}16\times10^{3})$	$6{\cdot}40$ $(9{\cdot}93\times10^{2})$	$-1{\cdot}14\times10^{3}$ $(9{\cdot}00\times10^{2})$
5	$6{\cdot}01\times10^{2}$ $(3{\cdot}38\times10^{2})$	$1{\cdot}14\times10^{3}$ $(1{\cdot}08\times10^{3})$	$-9{\cdot}99\times10^{2}$ $(1{\cdot}26\times10^{3})$	$2{\cdot}21\times10^{3}$ $(1{\cdot}57\times10^{3})$	$1{\cdot}27\times10^{3}$ $(1{\cdot}39\times10^{3})$	$-6{\cdot}64\times10^{2}$ $(1{\cdot}72\times10^{3})$	$-8{\cdot}98\times10^{2}$ $(1{\cdot}02\times10^{3})$	$-5{\cdot}17\times10^{2}$ $(8{\cdot}87\times10^{2})$	$-1{\cdot}06\times10^{3}$ $(1{\cdot}13\times10^{3})$	$-1{\cdot}05\times10^{3}$ $(1{\cdot}10\times10^{3})$
6	$-4{\cdot}63\times10^{2}$ $(2{\cdot}73\times10^{2})$	$-2{\cdot}87\times10^{-1}$ $(1{\cdot}00\times10^{3})$	$-9{\cdot}07\times10^{2}$ $(1{\cdot}26\times10^{3})$	$3{\cdot}23\times10^{3}$ $(1{\cdot}66\times10^{3})$	$8{\cdot}39\times10^{2}$ $(1{\cdot}30\times10^{3})$	$-8{\cdot}98\times10^{2}$ $(1{\cdot}02\times10^{3})$	$1{\cdot}80\times10^{3}$ $(1{\cdot}08\times10^{3})$	$-1{\cdot}69\times10^{3}$ $(9{\cdot}03\times10^{2})$	$-1{\cdot}46\times10^{2}$ $(1{\cdot}01\times10^{3})$	$1{\cdot}34\times10^{3}$ $(7{\cdot}80\times10^{2})$
7	$5{\cdot}37\times10^{2}$ $(3{\cdot}08\times10^{2})$	$2{\cdot}29\times10^{3}$ $(1{\cdot}14\times10^{3})$	$1{\cdot}18\times10^{3}$ $(1{\cdot}16\times10^{3})$	$2{\cdot}53\times10^{3}$ $(1{\cdot}29\times10^{3})$	$-1{\cdot}83\times10^{3}$ $(1{\cdot}16\times10^{3})$	$-5{\cdot}17\times10^{2}$ $(8{\cdot}87\times10^{2})$	$-1{\cdot}69\times10^{3}$ $(9{\cdot}03\times10^{2})$	$-7{\cdot}98\times10^{2}$ $(1{\cdot}19\times10^{3})$	$-3{\cdot}98\times10^{1}$ $(9{\cdot}97\times10^{2})$	$4{\cdot}55\times10^{2}$ $(1{\cdot}31\times10^{2})$
8	$-4{\cdot}56\times10^{2}$ $(2{\cdot}88\times10^{2})$	$6{\cdot}80\times10^{2}$ $(1{\cdot}14\times10^{3})$	$1{\cdot}00\times10^{3}$ $(9{\cdot}82\times10^{2})$	$2{\cdot}02\times10^{3}$ $(9{\cdot}67\times10^{2})$	$6{\cdot}40$ $(9{\cdot}93\times10^{2})$	$-1{\cdot}06\times10^{3}$ $(1{\cdot}12\times10^{3})$	$-1{\cdot}46\times10^{2}$ $(1{\cdot}01\times10^{3})$	$-3{\cdot}98\times10^{1}$ $(9{\cdot}96\times10^{2})$	$1{\cdot}49\times10^{3}$ $(2{\cdot}07\times10^{3})$	$3{\cdot}12\times10^{3}$ $(1{\cdot}98\times10^{3})$
9	$-5{\cdot}95\times10^{1}$ $(2{\cdot}92\times10^{2})$	$9{\cdot}86\times10^{2}$ $(7{\cdot}84\times10^{2})$	$1{\cdot}67\times10^{2}$ $(1{\cdot}04\times10^{3})$	$7{\cdot}58\times10^{2}$ $(9{\cdot}78\times10^{2})$	$-1{\cdot}14\times10^{3}$ $(9{\cdot}00\times10^{2})$	$-1{\cdot}05\times10^{3}$ $(1{\cdot}10\times10^{3})$	$1{\cdot}34\times10^{3}$ $(7{\cdot}80\times10^{2})$	$4{\cdot}55\times10^{2}$ $(1{\cdot}31\times10^{3})$	$3{\cdot}12\times10^{3}$ $(1{\cdot}98\times10^{3})$	$-6{\cdot}07\times10^{2}$ $(1{\cdot}82\times10)^{3}$

TABLE 2. Estimated imaginary part of bispectrum of velocity derivative (record 301–400).
Estimated standard deviation in parentheses. One unit in frequency is 15·276 Hz.

Frequency	0	2	4	6	8
0	$-1{\cdot}82\times10^{3}$ ($2{\cdot}50\times10^{2}$)	$-3{\cdot}74\times10^{3}$ ($4{\cdot}67\times10^{2}$)	$-2{\cdot}39\times10^{3}$ ($3{\cdot}82\times10^{2}$)	$-1{\cdot}97\times10^{3}$ ($4{\cdot}46\times10^{2}$)	$-2{\cdot}04\times10^{3}$ ($4{\cdot}62\times10^{2}$)
2	$-3{\cdot}74\times10^{3}$ ($4{\cdot}67\times10^{2}$)	$-3{\cdot}26\times10^{3}$ ($6{\cdot}48\times10^{2}$)	$-3{\cdot}41\times10^{3}$ ($5{\cdot}05\times10^{2}$)	$-2{\cdot}19\times10^{3}$ ($4{\cdot}97\times10^{2}$)	$-3{\cdot}19\times10^{3}$ ($5{\cdot}09\times10^{2}$)
4	$-2{\cdot}39\times10^{3}$ ($3{\cdot}82\times10^{2}$)	$-3{\cdot}41\times10^{3}$ ($5{\cdot}05\times10^{2}$)	$-3{\cdot}31\times10^{3}$ ($7{\cdot}05\times10^{2}$)	$-2{\cdot}67\times10^{3}$ ($4{\cdot}70\times10^{2}$)	$-2{\cdot}11\times10^{3}$ ($4{\cdot}46\times10^{2}$)
6	$-1{\cdot}97\times10^{3}$ ($4{\cdot}46\times10^{2}$)	$-2{\cdot}19\times10^{3}$ ($4{\cdot}97\times10^{2}$)	$-2{\cdot}67\times10^{3}$ ($4{\cdot}70\times10^{2}$)	$-3{\cdot}00\times10^{3}$ ($6{\cdot}12\times10^{2}$)	$-1{\cdot}99\times10^{3}$ ($5{\cdot}02\times10^{2}$)
8	$-2{\cdot}04\times10^{3}$ ($4{\cdot}62\times10^{2}$)	$-3{\cdot}19\times10^{3}$ ($5{\cdot}09\times10^{2}$)	$-2{\cdot}11\times10^{3}$ ($4{\cdot}46\times10^{2}$)	$-1{\cdot}99\times10^{3}$ ($5{\cdot}02\times10^{2}$)	$-1{\cdot}89\times10^{3}$ ($5{\cdot}43\times10^{2}$)

TABLE 3. Estimated real part of bispectrum of velocity derivative (record 101–700). Estimated standard deviation in parentheses. One unit in frequency is 15·276 Hz.

Frequency	0	2	4	6	8
0	$-1{\cdot}62\times10^{1}$ ($1{\cdot}26\times10^{2}$)	$3{\cdot}19\times10^{1}$ ($1{\cdot}19\times10^{2}$)	$-2{\cdot}90\times10^{2}$ ($1{\cdot}31\times10^{2}$)	8·73 ($1{\cdot}33\times10^{2}$)	$-1{\cdot}75\times10^{2}$ ($1{\cdot}09\times10^{2}$)
2	$3{\cdot}19\times10^{1}$ ($1{\cdot}19\times10^{2}$)	$7{\cdot}92\times10^{2}$ (6.21×10^{2})	$-1{\cdot}38\times10^{1}$ ($4{\cdot}77\times10^{2}$)	$3{\cdot}67\times10^{2}$ ($4{\cdot}40\times10^{2}$)	$4{\cdot}39\times10^{2}$ ($4{\cdot}02\times10^{2}$)
4	$-2{\cdot}90\times10^{2}$ ($1{\cdot}31\times10^{2}$)	$-1{\cdot}38\times10^{1}$ ($4{\cdot}77\times10^{2}$)	$3{\cdot}27\times10^{2}$ ($7{\cdot}40\times10^{2}$)	$-2{\cdot}27\times10^{2}$ ($5{\cdot}02\times10^{2}$)	$-4{\cdot}48\times10^{1}$ ($3{\cdot}68\times10^{2}$)
6	8·73 ($1{\cdot}33\times10^{2}$)	$3{\cdot}67\times10^{2}$ ($4{\cdot}40\times10^{2}$)	$-2{\cdot}27\times10^{2}$ ($5{\cdot}02\times10^{2}$)	$5{\cdot}67\times10^{2}$ ($6{\cdot}89\times10^{2}$)	$-5{\cdot}87\times10^{2}$ ($4{\cdot}42\times10^{2}$)
8	$-1{\cdot}75\times10^{2}$ ($1{\cdot}09\times10^{2}$)	$4{\cdot}39\times10^{2}$ ($4{\cdot}02\times10^{2}$)	$-4{\cdot}48\times10^{1}$ ($3{\cdot}68\times10^{2}$)	$-5{\cdot}87\times10^{2}$ ($4{\cdot}42\times10^{2}$)	$3{\cdot}67\times10^{2}$ ($6{\cdot}14\times10^{2}$)

TABLE 4. Estimated imaginary part of bispectrum of velocity derivative (record 101–700). Estimated standard deviation in parentheses. One unit in frequency is 15·276 Hz.

(4) To reduce the variance, we averaged, at each (λ_1, λ_2), within a square neighbourhood 31×31, i.e. for the kth record,

$$\bar{b}_k(\lambda_1, \lambda_2) = \frac{1}{961} \sum_{j_1=\lambda_1-15}^{\lambda_1+15} \sum_{j_2=\lambda_2-15}^{\lambda_2+15} b(j_1, j_2).$$

(5) To reduce the variance further, we averaged 100 records to get our estimates

$$\bar{\bar{b}}_1(\lambda_1, \lambda_2) = \frac{1}{100} \sum_{k=301}^{400} \bar{b}_k(\lambda_1, \lambda_2).$$

We also computed the variance of this estimate at a few selected points. The procedures were as follows.

(i) Repeat steps 1–4 in the computation of the bispectrum estimate for each kth record to get $\bar{b}(\lambda_1, \lambda_2)$.

Frequency	0	2	4	6	8
0	−0·89	−0·91	−0·49	−0·44	−0·54
2	−0·91	−0·51	−0·52	−0·38	−0·67
4	−0·49	−0·52	−0·51	−0·48	−0·47
6	−0·44	−0·38	−0·48	−0·63	−0·56
8	−0·54	−0·67	−0·47	−0·56	−0·71

TABLE 5. Normalized estimated real part of bispectrum of velocity derivative (record 101–700). One unit in frequency is 15·276 Hz.

(ii) Compute

$$\mathrm{Var}\,(\lambda_1, \lambda_2) = \frac{1}{100} \sum_{k=301}^{400} [\mathrm{Re}\,\bar{b}_k(\lambda_1, \lambda_2) - \mathrm{Re}\,\bar{\bar{b}}_1(\lambda_1, \lambda_2)]^2$$

and the corresponding variance for the imaginary part.

(iii) Compute $\mathrm{SD}(\lambda_1, \lambda_2) = [\frac{1}{100}\,\mathrm{var}(\lambda_1, \lambda_2)]^{\frac{1}{2}}$ for both real and imaginary parts. This gave us the standard deviation of our estimates.

The appendix gives results determining the large-sample behaviour of estimates. From the theorem in the appendix, it is clear that to first order the variance of the third-order periodogram is proportional to the sample size. Consistent with the low wavenumber range over which one wishes to estimate, it is clear that one does not want to process too much data in computing fast Fourier transforms. Otherwise, to reduce the variance we should have to smooth the periodogram (third order) extensively and this would be inconvenient since there is great expense involved in moving information in and out of the large core memory of the computer. Further, one would increase bias. For these reasons it seemed best to follow the computational procedure indicated in steps 1–5.

It should be noted that the standard deviation of the final estimate of the bispectra based on the asymptotic results of the appendix is of the same order of magnitude as the standard deviation estimated from the data. The computations in tables 1–4 should be thought of on a relative rather than an absolute scale. One unit in frequency in these tables is 15·276 Hz. In table 5 the normalized estimated real part of the bispectrum has been computed, i.e.

$$\mathrm{Re}\,b(\lambda_1, \lambda_2)/\{f(\lambda_1) f(\lambda_2) f(\lambda_1 + \lambda_2)\}^{\frac{1}{2}}.$$

Of course, estimates of $\mathrm{Re}\,b(\lambda_1, \lambda_2)$ and of the spectral density f are inserted. An additional multiplicative factor of $8^2 = 64$ is put in since the bispectrum computed has been derived by initially averaging data over disjoint blocks of 8 successive readings. This averaging of data has introduced also a multiplicative factor for the bispectrum due to the filtering which has the form

$$\frac{1}{8^3} \frac{\sin 4\alpha_1}{\sin \frac{1}{2}\alpha_1} \frac{\sin 4\alpha_2}{\sin \frac{1}{2}\alpha_2} \frac{\sin 4(\alpha_1 + \alpha_2)}{\sin \frac{1}{2}(\alpha_1 + \alpha_2)},$$

where $\alpha_i = \lambda_i \pi / 2086$, $i = 1, 2$, and the λ_i are in Hz. Table 6 gives this factor for the range of pairs of frequencies of interest. The numbers obtained in tables 1–4 should be divided by the appropriate factor in this table.

Frequency	0	1	2	3	4	5	6	7	8	9
0	1·00	$9·97 \times 10^{-1}$	$9·89 \times 10^{-1}$	$9·75 \times 10^{-1}$	$9·56 \times 10^{-1}$	$9·32 \times 10^{-1}$	$9·04 \times 10^{-1}$	$8·71 \times 10^{-1}$	$8·34 \times 10^{-1}$	$7·97 \times 10^{-1}$
1	$9·97 \times 10^{-1}$	$9·92 \times 10^{-1}$	$9·81 \times 10^{-1}$	$9·64 \times 10^{-1}$	$9·43 \times 10^{-1}$	$9·17 \times 10^{-1}$	$8·86 \times 10^{-1}$	$8·51 \times 10^{-1}$	$8·13 \times 10^{-1}$	$7·71 \times 10^{-1}$
2	$9·89 \times 10^{-1}$	$9·81 \times 10^{-1}$	$9·67 \times 10^{-1}$	$9·48 \times 10^{-1}$	$9·25 \times 10^{-1}$	$8·96 \times 10^{-1}$	$8·63 \times 10^{-1}$	$8·27 \times 10^{-1}$	$7·87 \times 10^{-1}$	$7·44 \times 10^{-1}$
3	$9·75 \times 10^{-1}$	$9·64 \times 10^{-1}$	$9·48 \times 10^{-1}$	$9·27 \times 10^{-1}$	$9·01 \times 10^{-1}$	$8·71 \times 10^{-1}$	$8·37 \times 10^{-1}$	$7·99 \times 10^{-1}$	$7·58 \times 10^{-1}$	$7·14 \times 10^{-1}$
4	$9·56 \times 10^{-1}$	$9·43 \times 10^{-1}$	$9·25 \times 10^{-1}$	$9·01 \times 10^{-1}$	$8·73 \times 10^{-1}$	$8·41 \times 10^{-1}$	$8·06 \times 10^{-1}$	$7·67 \times 10^{-1}$	$7·25 \times 10^{-1}$	$6·80 \times 10^{-1}$
5	$9·32 \times 10^{-1}$	$9·17 \times 10^{-1}$	$8·96 \times 10^{-1}$	$8·71 \times 10^{-1}$	$8·41 \times 10^{-1}$	$8·08 \times 10^{-1}$	$7·71 \times 10^{-1}$	$7·31 \times 10^{-1}$	$6·89 \times 10^{-1}$	$6·44 \times 10^{-1}$
6	$9·04 \times 10^{-1}$	$8·86 \times 10^{-1}$	$8·63 \times 10^{-1}$	$8·37 \times 10^{-1}$	$8·06 \times 10^{-1}$	$7·71 \times 10^{-1}$	$7·33 \times 10^{-1}$	$6·93 \times 10^{-1}$	$6·50 \times 10^{-1}$	$6·06 \times 10^{-1}$
7	$8·71 \times 10^{-1}$	$8·51 \times 10^{-1}$	$8·27 \times 10^{-1}$	$7·99 \times 10^{-1}$	$7·67 \times 10^{-1}$	$7·31 \times 10^{-1}$	$6·93 \times 10^{-1}$	$6·52 \times 10^{-1}$	$6·09 \times 10^{-1}$	$5·65 \times 10^{-1}$
8	$8·34 \times 10^{-1}$	$8·13 \times 10^{-1}$	$7·87 \times 10^{-1}$	$7·58 \times 10^{-1}$	$7·25 \times 10^{-1}$	$6·89 \times 10^{-1}$	$6·50 \times 10^{-1}$	$6·09 \times 10^{-1}$	$5·67 \times 10^{-1}$	$5·23 \times 10^{-1}$
9	$7·94 \times 10^{-1}$	$7·71 \times 10^{-1}$	$7·44 \times 10^{-1}$	$7·14 \times 10^{-1}$	$6·80 \times 10^{-1}$	$6·44 \times 10^{-1}$	$6·06 \times 10^{-1}$	$5·65 \times 10^{-1}$	$5·23 \times 10^{-1}$	$4·81 \times 10^{-1}$

TABLE 6. Multiplicative factor due to filtering.
One unit in frequency is 15·276 Hz.

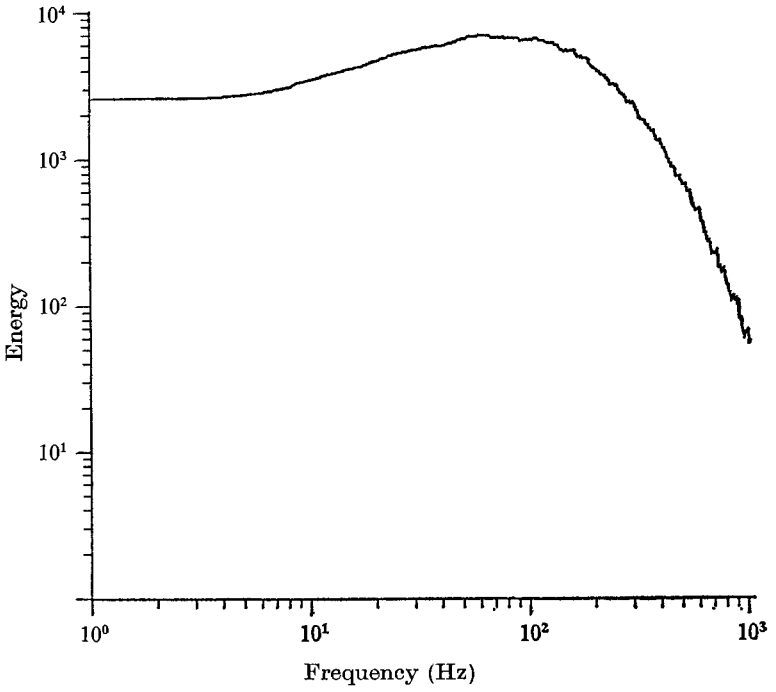

FIGURE 1. Estimated spectral density (record 301–400) of the velocity derivative: log–log plot

5. Results of the computation

A log–log plot of the estimated spectral density of the velocity derivative is given in figure 1. Notice that dealing with the derivative has effectively whitened (approximately) the spectral density over the inertial range, roughly from 1 to 100 Hz. The estimated density varies between 2×10^3 and 8×10^3 for frequencies from 1 to 150 Hz. In table 1 the estimated real part of the bispectrum of the velocity derivative is given together with estimates of the standard deviation locally. The bispectrum is negative for all values of λ_1 and λ_2 computed (between 1 and 150 Hz). It is largest in magnitude for λ_1 and λ_2 small, particularly about the diagonal, and decreases slowly in magnitude as λ_1 and λ_2 increase. The estimated standard deviation ranges from one-third to one-fifth of the magnitude of the bispectrum when λ_1 and λ_2 are between 1 and 90 Hz. This and the relatively smooth variation of the real part of the bispectrum indicate that we are getting reasonable statistical resolution of the estimate. Notice, on the other hand, that in table 2 the estimated imaginary part of the bispectrum oscillates from positive to negative values consistent with the bandwidth of the smoothing weights two-dimensionally. The magnitude of the estimated imaginary part of the bispectrum is less than that of the real part, often about a tenth the size. Further, the estimated standard deviation locally is about the same size as the imaginary part itself. This suggests that the imaginary part is probably zero over most of the range. For homogeneous (locally) isotropic turbulence it

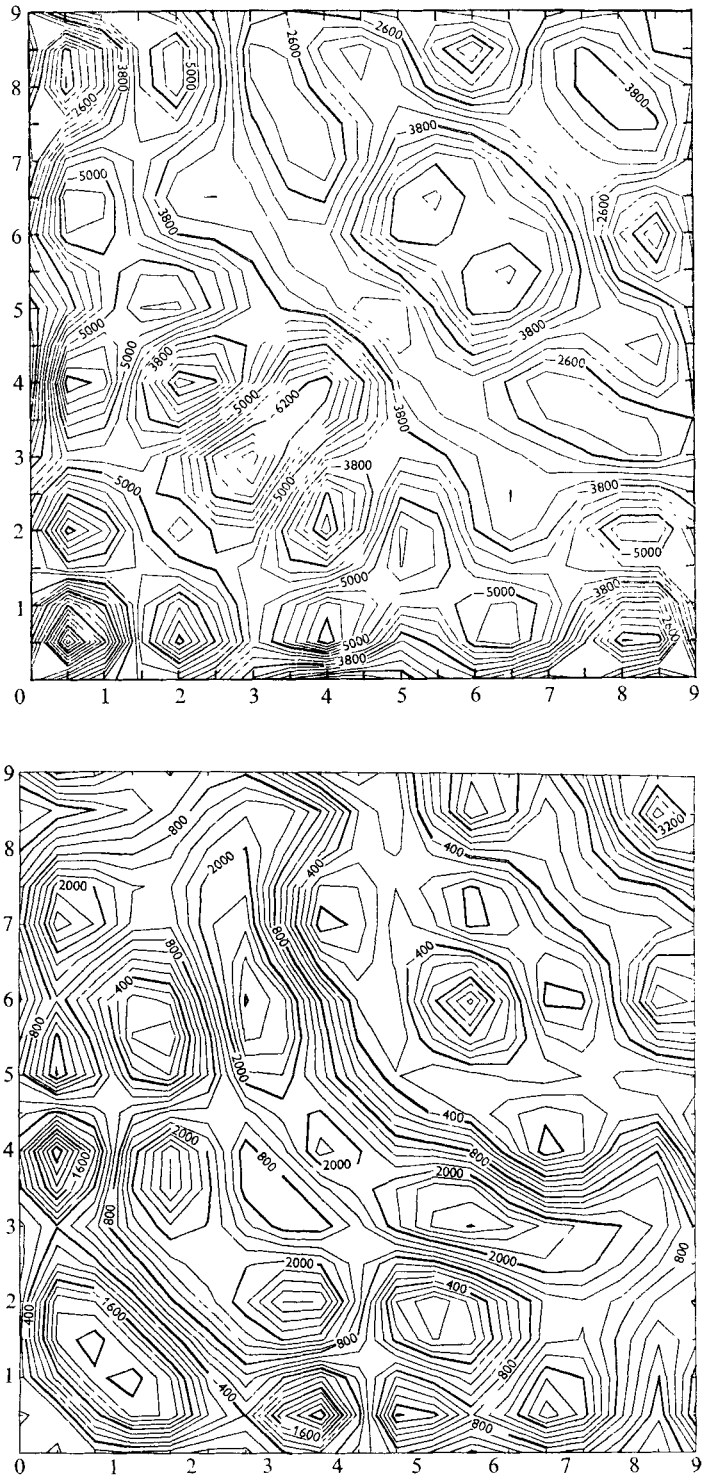

FIGURE 2. Level-surface plots corresponding to (*a*) table 1 and (*b*) table 2

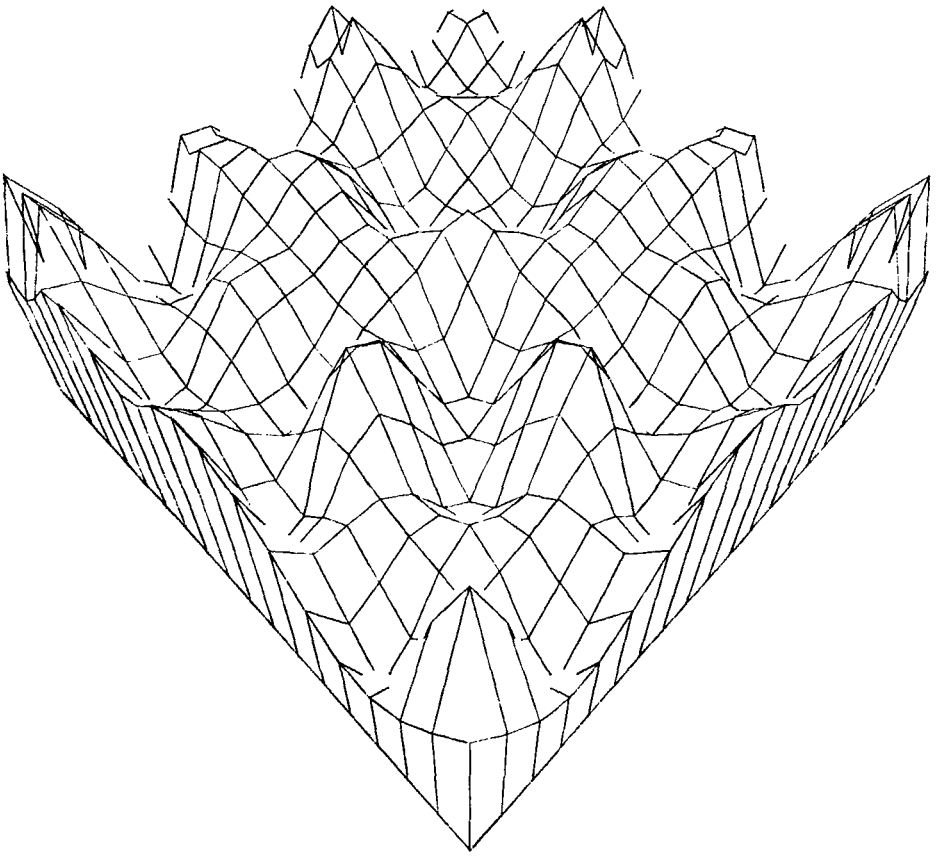

FIGURE 3. Perspective view of figure 2(*a*).

would be zero. Notice that the real part of the bispectrum determines one of the nine terms that specify $q(k_1, k_1')$ in (12), namely

$$k_1 E\{dz(k_1 - k_1')\, dz(-k_1)\, dz(k_1')\}.$$

We actually estimate $b(w_1, w_1')$, where $w_1 = k_1 - k_1' > 0$ and $w_1' = k_1' > 0$, and this corresponds to a transfer of energy (or vorticity) from $k_1' = w_1'$ to

$$k_1 = w_1 + w_1' > k_1'.$$

It clearly would be of interest to have an experiment set-up, for example in a wind tunnel, where the other eight types of term could be measured.

The computations suggest that contributions of wavenumber triplets to spectral transfer and the rate of vorticity production are non-local in wavenumber and comparable over the whole range of wavenumbers studied. Physically this would indicate that on the average vortices of broadly different scales interact appreciably.

Strictly, the bispectrum at (λ_1, λ_2) with either λ_1 or $\lambda_2 = 0$ should be zero. However, we are actually estimating the average bispectrum over squares with a linear bandwidth of 7·638 Hz. It should be noted that there may be some effect

of aliasing at 100–150 Hz. The estimates in table 3 are a bit different from those in table 1 and can be attributed to some non-stationarity over the longer time range of records 101–700.

We thank John Wyngaard for the loan of the analog tape W-9. We are indebted to colleagues who read the manuscript and made helpful comments. This research was supported by the Office of Naval Research and the National Science Foundation.

Appendix. Bispectra and higher-order spectra

This appendix is concerned with a set of theoretical (statistical) results on the asymptotic behaviour of bispectral estimates. In our computations we were guided by these results in our averaging (in time) and smoothing (in frequency) so as to reduce the variance of the estimates. In fact, it is clear that without these theoretical results as a guide we should have obtained no resolvability in our estimates.

It will be convenient at this point to consider $X(t)$, $t = \ldots, -1, 0, 1, \ldots$, a discrete-time-parameter *stationary process all of whose moments exist.* Then, assuming $EX(t) \equiv 0$ and $X(t)$ to be real valued,

$$\begin{aligned} X(t) &= \int_{-\pi}^{\pi} e^{it\lambda}\, dz(\lambda) \\ &= \int_0^{\pi} \cos t\lambda\, dz^{(1)}(\lambda) + \int_0^{\pi} \sin t\lambda\, dz^{(2)}(\lambda), \end{aligned}$$

where

$$dz(\lambda) = \overline{dz(-\lambda)}, \quad dz^{(1)}(\lambda) = 2\,\mathrm{Re}\, dz(\lambda), \quad dz^{(2)}(\lambda) = -2\,\mathrm{Im}\, dz(\lambda).$$

Notice that, if the cumulant

$$c(t_1, t_2, \ldots, t_k) = \mathrm{cum}\,(X(t_1), \ldots, X(t_k)),$$

then $c(t_1, t_2, \ldots, t_k)$ depends only on $t_2 - t_1, \ldots, t_k - t_1$ because of the stationarity of the process $X(t)$. The cumulant $c(t_1, t_2, \ldots, t_k)$ is a kth-order polynomial in moments of order no higher than k. Conversely the kth-order moment $E\{X(t_1) \ldots X(t_k)\}$ is a kth-order polynomial in cumulants of order no higher than k. We *assume summability of c as a function of $k-1$ of its arguments.*

This summability is a sort of mixing condition for the random process $X(t)$. It implies an approach to independence of groups of random variables separated by greater time gaps. This implies that kth-order cumulant spectral densities

$${}_kf(\lambda_1, \lambda_2, \ldots, \lambda_k) = (2\pi)^{-k+1} \sum_{v_1, \ldots, v_{k-1}} c(0, v_1, v_2, \ldots, v_{k-1}) \exp\left(-i \sum_1^{k-1} v_j \lambda_j\right)$$

exist, where it is understood that

$$\sum_{j=1}^{k} \lambda_j \equiv 0 \quad \text{modulo } 2\pi.$$

Notice that the second- and third-order spectral densities can be written in terms of moments rather than cumulants. Now

$$Edz(\lambda)\,\overline{dz(\mu)} = \delta(\lambda-\mu)f(\lambda)\,d\lambda, \quad -\pi < \lambda, \quad \mu \leqslant \pi,$$
$$Edz^{(j)}(\lambda)\,dz^{(k)}(\mu) = \delta(\lambda-\mu)\,\delta_{j,k}\,{}_2f(\lambda)\,d\lambda,$$

where $f(\lambda) = {}_2f(\lambda, -\lambda)$. Further

$$Edz(\lambda_1)\,dz(\lambda_2)\ldots dz(\lambda_k) = \eta(\lambda_1+\lambda_2+\ldots+\lambda_k)\,{}_kf(\lambda_1,\lambda_2,\ldots,\lambda_k)\,d\lambda_1\ldots d\lambda_k,$$

where
$$\eta(\lambda) = \sum_j \delta(\lambda+2j\pi).$$

Because $X(t)$ is real valued

$${}_kf(\lambda_1,\ldots,\lambda_k) = \overline{{}_kf(-\lambda_1,\ldots,-\lambda_k)}$$

and so

$$c(\lambda_1,\ldots,\lambda_k) = c(-\lambda_1,\ldots,-\lambda_k), \quad q(\lambda_1\ldots,\lambda_k) = -q(-\lambda_1,\ldots,-\lambda_k),$$

where c and q are the real and imaginary parts of f.

Let
$$d_N(\lambda) = \sum_{t=0}^{N-1} X(t)e^{it\lambda}$$

be the Fourier transform of the finite section $\{X(t)|0 \leqslant t < N\}$. Estimates of the kth-order spectra are often constructed in terms of the following kth-order analogue of the second-order periodogram:

$$I^{(N)}(\lambda_1,\ldots,\lambda_k) = (2\pi)^{-k+1}N^{-1}\prod_{j=1}^{k} d^{(N)}(\lambda_j),$$

where
$$\sum_{j=1}^{k}\lambda_j \equiv 0 \pmod{2\pi}.$$

For this reason, it is of some interest to get a good approximation for the variance (and covariances) of these statistics. The following result is helpful in obtaining such approximations.

Let $X(t)$ be a strictly stationary sequence with continuously differentiable spectral density. Then

$$\operatorname{cov}(\operatorname{Re} d_N(\lambda), \operatorname{Re} d_N(\mu)) = [f(\lambda)f(\mu)]^{\frac{1}{2}}\pi\left\{\operatorname{Re}\frac{e^{iN(\lambda-\mu)}-1}{e^{i(\lambda-\mu)}-1} + \operatorname{Re}\frac{e^{iN(\lambda+\mu)}-1}{e^{i(\lambda+\mu)}-1}\right\} + O(\log N),$$

$$\operatorname{cov}(\operatorname{Im} d_N(\lambda), \operatorname{Im} d_N(\mu)) = [f(\lambda)f(\mu)]^{\frac{1}{2}}\pi\left\{\operatorname{Re}\frac{e^{iN(\lambda-\mu)}-1}{e^{i(\lambda-\mu)}-1} - \operatorname{Re}\frac{e^{iN(\lambda+\mu)}-1}{e^{i(\lambda+\mu)}-1}\right\} + O(\log N),$$

$$\operatorname{cov}(\operatorname{Re} d_N(\lambda), \operatorname{Im} d_N(\mu)) = [f(\lambda)f(\mu)]^{\frac{1}{2}}\pi\left\{\operatorname{Im}\frac{e^{iN(\lambda+\mu)}-1}{e^{i(\lambda+\mu)}-1} - \operatorname{Im}\frac{e^{iN(\lambda-\mu)}-1}{e^{i(\lambda-\mu)}-1}\right\} + O(\log N).$$

The result follows by noting that

$$\operatorname{cov}(d_N(\lambda), d_N(\mu)) = E[d_N(\lambda)\,d_N(\mu)]$$
$$= E\left\{\int_{-\pi}^{\pi}\sum_{t=0}^{N-1} e^{it(\alpha+\lambda)}dz(\alpha)\int_{-\pi}^{\pi}\sum_{t=0}^{N-1} e^{-it(\alpha-\mu)}\overline{dz(\alpha)}\right\}$$
$$= E\left\{\int_{-\pi}^{\pi}\frac{e^{iN(\alpha+\lambda)}-1}{e^{i(\alpha+\lambda)}-1}dz(\alpha)\int_{-\pi}^{\pi}\frac{e^{-iN(\alpha-\mu)}-1}{e^{-i(\alpha-\mu)}-1}\overline{dz(\alpha)}\right\}$$

and by using an approximation like that in Rosenblatt (1974, p. 174) leading to

$$[f(\lambda)f(\mu)]^{\frac{1}{2}} 2\pi \frac{e^{iN(\lambda+\mu)}-1}{e^{i(\lambda-\mu)}-1} + O(\log N).$$

Notice that $d_N(\lambda)$ is a discrete time-truncated Fourier transform of the data $X(t)$, $t = 0, \ldots, N-1$. The result implies that the random variables

$$N^{-\frac{1}{2}} \operatorname{Re} d_N(\lambda_j), \quad N^{-\frac{1}{2}} \operatorname{Im} d_N(\lambda_j), \quad \lambda_j = 2\pi j/N, \quad j = 1, \ldots, N-1,$$

for large N approximately have variance $\pi f(\lambda_j)$, and are asymptotically uncorrelated. In fact, under appropriate conditions one can show these random variables are for large N approximately jointly Gaussian.

The periodogram

$$(2\pi N)^{-1}|d_N(\lambda_j)|^2 = I_N(\lambda_j)$$

is a poor estimate of $f(\lambda_j)$. Its mean

$$EI_N(\lambda_j) \cong f(\lambda_j)$$

is approximately $f(\lambda_j)$ but its variance

$$\operatorname{var}(I_N(\lambda_j)) \cong f^2(\lambda_j), \quad j = 1, \ldots, N,$$

does not tend to zero as $N \to \infty$. If one has M disjoint blocks of N successive observations, a periodogram $I_N^{(s)}(\lambda_j)$, $s = 1, \ldots, M$, can be estimated from each block. By taking the average of these periodograms

$$\frac{1}{M} \sum_{s=1}^{M} I_N^{(s)}(\lambda_j) = f^{(1)}(\lambda_j),$$

one gets an estimate $f^{(1)}(\lambda_j)$ with the same approximate mean $f(\lambda_j)$ and reduced variance $\pi M^{-1} f^2(\lambda_j)$, approximately. This is an average over time sections. The variance can be reduced further by spatial averaging over wavenumbers. Thus a second estimate

$$f^{(2)}(\lambda_j) = \frac{1}{2r+1} \sum_{u=s-r}^{s+r} f^{(1)}(\lambda_u)$$

has approximate variance

$$\frac{\pi}{M(2r+1)} f^2(\lambda_j).$$

However, this averaging over wavenumbers must not be made too broad for then the mean of the estimate would no longer be approximately $f(\lambda_j)$ (the bias of the estimate would become large).

A detailed argument for the computation of the variance and covariance will be carried out for the bispectral (third-order) periodogram. A corresponding analysis can be carried out for a kth-order periodogram with $k > 3$. First notice that

$$\begin{aligned}\operatorname{Re}\{d_N(\lambda)\, d_N(\mu)\, d_N(-\lambda-\mu)\} = {} & \operatorname{Re} d_N(\lambda) \operatorname{Re} d_N(\mu) \operatorname{Re} d_N(\lambda+\mu) \\ & + \operatorname{Re} d_N(\lambda) \operatorname{Im} d_N(\mu) \operatorname{Im} d_N(\lambda+\mu) \\ & + \operatorname{Im} d_N(\lambda) \operatorname{Re} d_N(\mu) \operatorname{Im} d_N(\lambda+\mu) \\ & - \operatorname{Im} d_N(\lambda) \operatorname{Im} d_N(\mu) \operatorname{Re} d_N(\lambda+\mu)\end{aligned}$$

and

$$\begin{aligned}\operatorname{Im}\{d_N(\lambda)\,d_N(\mu)\,d_N(-\lambda-\mu)\} = {} & \operatorname{Im} d_N(\lambda)\operatorname{Im} d_N(\mu)\operatorname{Im} d_N(\lambda+\mu)\\ & -\operatorname{Re} d_N(\lambda)\operatorname{Re} d_N(\mu)\operatorname{Im} d_N(\lambda+\mu)\\ & +\operatorname{Re} d_N(\lambda)\operatorname{Im} d_N(\mu)\operatorname{Re} d_N(\lambda+\mu)\\ & +\operatorname{Im} d_N(\lambda)\operatorname{Re} d_N(\mu)\operatorname{Re} d_N(\lambda+\mu).\end{aligned}$$

One can obtain the following result. *Let $X(t)$ be a strictly stationary process with kth cumulant functions up to sixth order all summable as functions of $k-1$ variables. Let s_1, s_2, l_1 and l_2 be integers with $0 < s_1 < s_2$ and $0 < l_1 < l_2$. Then*

$$\begin{aligned}&\operatorname{cov}\left(\operatorname{Re}\left\{\frac{1}{(2\pi)^2N}d_N\left(\frac{2\pi s_1}{N}\right)d_N\left(\frac{2\pi s_2}{N}\right)d_N\left(-\frac{2\pi(s_1+s_2)}{N}\right)\right\},\right.\\ &\qquad\left.\operatorname{Re}\left\{\frac{1}{(2\pi)^2N}d_N\left(\frac{2\pi l_1}{N}\right)d_N\left(\frac{2\pi l_2}{N}\right)d_N\left(-\frac{2\pi(l_1+l_2)}{N}\right)\right\}\right)\\ &= \frac{N}{4\pi}f\left(\frac{2\pi s_1}{N}\right)f\left(\frac{2\pi s_2}{N}\right)f\left(\frac{2\pi(s_1+s_2)}{N}\right)\delta_{s_1,l_1}\delta_{s_2,l_2}+O(\log N)^2\\ &= \operatorname{cov}\left(\operatorname{Im}\left\{\frac{1}{(2\pi)^2N}d_N\left(\frac{2\pi s_1}{N}\right)d_N\left(\frac{2\pi s_2}{N}\right)d_N\left(-\frac{2\pi(s_1+s_2)}{N}\right)\right\},\right.\\ &\qquad\left.\operatorname{Im}\left\{\frac{1}{(2\pi)^2N}d_N\left(\frac{2\pi l_1}{N}\right)d_N\left(\frac{2\pi l_2}{N}\right)d_N\left(-\frac{2\pi(l_1+l_2)}{N}\right)\right\}\right),\end{aligned}$$

while

$$\begin{aligned}&\operatorname{cov}\left(\operatorname{Re}\left\{\frac{1}{(2\pi)^2N}d_N\left(\frac{2\pi s_1}{N}\right)d_N\left(\frac{2\pi s_2}{N}\right)d_N\left(-\frac{2\pi(s_1+s_2)}{N}\right)\right\},\right.\\ &\qquad\left.\operatorname{Im}\left\{\frac{1}{(2\pi)^2N}d_N\left(\frac{2\pi l_1}{N}\right)d_N\left(\frac{2\pi l_2}{N}\right)d_N\left(-\frac{2\pi(l_1+l_2)}{N}\right)\right\}\right) = O(\log N)^2.\end{aligned}$$

A more detailed discussion of some related questions can be found in Brillinger & Rosenblatt (1967) and Lumley & Takeuchi (1976).

One can use

$$(2\pi)^{-2}N^{-1}d_N(\lambda_1)\,d_N(\lambda_2)\,d_N(-\lambda_1-\lambda_2) = I_N(\lambda_1,\lambda_2)$$

as an analogue of the periodogram with respect to estimation of the bispectral density. It has the right approximate mean

$$EI_N(\lambda_1,\lambda_2) \cong b(\lambda_1,\lambda_2),$$

but its variance properties are much worse than those of the periodogram since

$$\operatorname{var}(\operatorname{Re} I_N(\lambda_1,\lambda_2)),\quad \operatorname{var}(\operatorname{Im} I_N(\lambda_1,\lambda_2)) \cong (N/4\pi)f(\lambda_1)f(\lambda_2)f(\lambda_1+\lambda_2),$$

so that the variance is proportional to the sample size. We were particularly interested in the inertial range (low wavenumbers) in our analysis and so it was because of this proportionality of the variance to sample size that the data was low-bandpass filtered by averaging every eight readings (see § 4). To reduce the variance of an estimate we have to average bispectral periodograms from disjoint time blocks (say M blocks) and then smooth spatially (over wavenumbers) to reduce the variance. This reduction of the variance by averaging $\operatorname{Re} I_N(\lambda_1,\lambda_2)$ and $\operatorname{Im} I_N(\lambda_1,\Lambda_2)$ over

$$\lambda_1 = 2\pi s_1/N,\quad \lambda_2 = 2\pi s_2/N,$$

$s_1, s_2 = 1, 2, \ldots, N-1$, follows from the asymptotically uncorrelated behaviour of the bispectral analogue of the periodogram of these points. Notice that an initial spectral estimate is essential in trying to gauge the magnitude of the variance of these estimates of the bispectrum.

REFERENCES

BATCHELOR, G. K. 1953 *The Theory of Homogeneous Turbulence.* Cambridge University Press.

BATCHELOR, G. K. & TOWNSEND, A. A. 1956 Turbulent diffusion. In *Surveys in Mechanics*, pp. 352–399. Cambridge University Press.

BETCHOV, R. 1956 An inequality concerning the production of vorticity in isotropic turbulence. *J. Fluid Mech.* **1**, 497–504.

BRILLINGER, D. R. & ROSENBLATT, M. 1967 Computation and interpretation of kth order spectra. In *Spectral Analysis of Time Series* (ed. B. Harris), pp. 189–232. Wiley.

CARTWRIGHT, D. E. 1968 A unified analysis of tides and surges round North and East Britain. *Phil. Trans.* A **263**, 1–55.

HASSELMAN, K., MUNK, W. & MACDONALD, G. 1963 Bispectra of ocean waves. In *Time Series Analysis* (ed. M. Rosenblatt), pp. 125–139. Wiley.

HAUGEN, D. A., KAIMAL, J. C. & BRADLEY, E. F. 1971 An experimental study of Reynolds stress and heat flux in the atmospheric boundary layer. *Quart. J. Roy. Met. Soc.* **97**, 1968.

HUBER, P. J., KLEINER, B., GASSER, TH. & DUMERMUTH, G. 1971 Statistical methods for investigating phase relations in stationary stochastic processes. *I.E.E.E. Trans. Audio Electroacoust.*

KÁRMÁN, T. VON 1937 The fundamentals of the statistical theory of turbulence. *J. Aero. Sci.* **4**, 131–138.

KRAICHNAN, R. H. 1959 The structure of isotropic turbulence at very high Reynolds numbers. *J. Fluid Mech.* **5**, 497–542.

KRAICHNAN, R. H. 1971 Inertial-range transfer in two- and three-dimensional turbulence. *J. Fluid Mech.* **47**, 525–535.

LUMLEY, J. L. & TAKEUCHI, K. 1976 Application of central-limit theorems to turbulence and higher-order spectra. *J. Fluid Mech.* **74**, 433–468.

RODEN, G. I. & BENDINER, D. J. 1973 Bispectra and cross-spectra of temperature, salinity, sound velocity and density functions with depth off Northeastern Japan. *J. Phys. Ocean.* **3**, 308–317.

ROSENBLATT, M. 1971 Curve estimates. *Ann. Math. Stat.* **42**, 1815–1842.

ROSENBLATT, M. 1974 *Random Processes.* Springer.

TAYLOR, G. I. 1938 Production and dissipation of vorticity in a turbulent fluid. *Proc. Roy. Soc.* A **144**, 15–23.

VAN ATTA, C. W. & YEH, T. T. 1973 The structure of internal intermittency in turbulent flows at large Reynolds number: experimental scale similarity. *J. Fluid Mech.* **59**, 537–559.

VAN ATTA, C. W. & YEH, T. T. 1975 Evidence for scale similarity of internal intermittency in turbulent flows at large Reynolds numbers. *J. Fluid Mech.* **71**, 417–440.

WYNGAARD, J. C. & LUMLEY, J. L. 1967 A sharp cutoff spectral differentiator. *J. Appl. Met.* **6**, 952.

WYNGAARD, J. C. & PAO, Y. H. 1972 Some measurements of the fine structure of large Reynolds number turbulence. In *Statistical Models and Turbulence, Lecture Notes in Physics*, vol. 12 (ed. M. Rosenblatt & C. Van Atta), pp. 384–401. Springer.

YEH, T. T. & VAN ATTA, C. W. 1973 Spectral transfer of scalar and velocity fields in heated-grid turbulence. *J. Fluid Mech.* **58**, 233–261.